Journal of Photochemistry and Photobiology A: Chemistry 211 (2010) 26–31

Contents lists available at ScienceDirect

Journal of Photochemistry and Photobiology A: Chemistry

journal homepage: www.elsevier.com/locate/jphotochem

Interlayer energy transfer between perylene diimide and phthalocyanine monolayers

Heli Lehtivuori[a,*], Tatu Kumpulainen[a], Alexander Efimov[a], Helge Lemmetyinen[a], Frank Würthner[b], Nikolai V. Tkachenko[a]

[a] Department of Chemistry and Bioengineering, Tampere University of Technology, P.O. Box 541, 33101 Tampere, Finland
[b] Universität Würzburg, Institut für Organische Chemie and Röntgen Research Center for Complex Material Systems, Am Hubland, 97074 Würzburg, Germany

ARTICLE INFO

Article history:
Received 13 October 2009
Received in revised form
31 December 2009
Accepted 25 January 2010
Available online 4 February 2010

Keywords:
Energy transfer
Fluorescence lifetime microscopy
Organized molecular films

ABSTRACT

Interlayer energy transfer from perylene diimide (PDI12) layers to phthalocyanine layers was studied using steady-state absorption, fluorescence, and time-resolved fluorescence and microscopy methods. The layers were prepared by Langmuir–Schäfer method, spaced by a few layers of octadecylamine deposited by Langmuir–Blodgett method, when required. The fluorescence lifetime microscopy method allowed to exclude defects from the energy transfer analysis and calculate the fluorescence lifetimes of PDI12 for the defect free areas. The estimated distance dependence of the interlayer energy transfer follows roughly second order dependences on the distance with the critical distance of 6.9 nm.

1. Introduction

As a traditional industrial pigment, perylene diimides (PDI) are used in many applications. In addition, PDI derivatives have been considered to be versatile and promising functional materials for organic-based electronic and optic devices, such as transistors and solar cells [1,2]. For solar cells it is necessary to have absorbance features that closely match the solar spectrum.

PDI derivatives possess intensive absorption in the visible part of the spectrum (400–600 nm) [3–6]. As materials for light-emitting diodes, solar cells, and transistors, PDI derivatives have attracted much attention due to their high thermal and chemical stabilities and good photoconductive properties [1,7].

Another important property of PDI derivatives is their ability to form different self-organized structures [8,9]. In particular, the PDI12 derivative, presented in Fig. 1, containing trialkylphenyl groups at the imide positions, has been thoroughly studied in a number of solvents at different concentrations and temperatures [5,6,10]. In nonpolar environment and films, the strong π–π interaction among the dyes produces well organized aggregates. The absorption and emission spectra of the aggregates are shifted drastically to the red, but the emission efficiency and lifetime remain rather high, which makes the aggregates promising structures for light harvesting and energy transfer applications. In this study, phthalocyanine (Pc) has been chosen as energy acceptor because of its rather high absorption in the red part of the spectrum (600–800 nm), thus providing required overlap between the emission spectrum of the donor and absorption spectrum of the acceptor. In addition phthalocyanines have electronic properties that make them suitable for applications in photovoltaic devices, molecular transistors, light-emitting devices, and other molecular electronics applications [11–15].

A number of methods have been used to prepare molecular films. In order to study intermolecular electron or energy transfers in solid state, the Langmuir–Blodgett (LB) and Langmuir–Schäfer (LS) techniques can be used to manufacture highly ordered molecular monolayers from amphiphilic molecules and deposit them onto solid substrates [16,17]. Even though PDI12 is not amphiphilic, it forms stable and smooth film at the air–water interface and the film can be transferred onto solid substrate by horizontal lifting (LS method) [6].

Photoinduced electron and energy transfer processes in organic materials such as perylene derivatives and phthalocyanines have been under intensive study during the past decade [7,19–23]. In our recent studies, PDI derivatives have been used as secondary electron acceptors in systems where the primary charge separation takes place in a porphyrin–fullerene or phthalocyanine–fullerene dyad molecules [24]. We have also observed that PDI derivative, similar to PDI12, donates energy to phthalocyanine–fullerene dyad after photoexcitation [25]. In the present study, dynamics and distance dependence of the intermolecular photoinduced energy transfer processes in PDI12|Pc bi-layer structure were studied.

* Corresponding author. Tel.: +358 3 3115 2002/3636; fax: +358 3 3115 2108.
E-mail address: heli.lehtivuori@tut.fi (H. Lehtivuori).

1010-6030/$ – see front matter © 2010 Elsevier B.V. All rights reserved.
doi:10.1016/j.jphotochem.2010.01.017

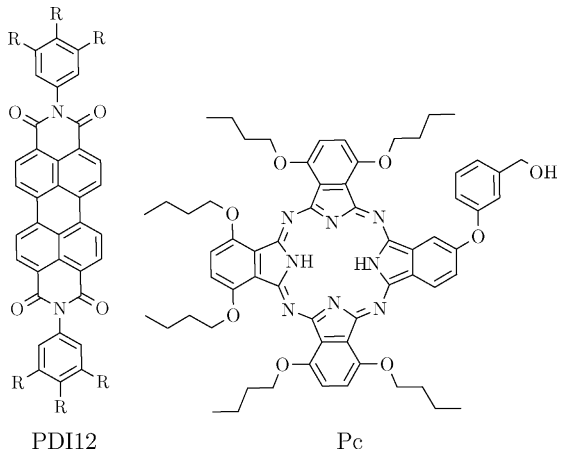

Fig. 1. Perylene diimide derivative (PDI12, where $R = C_{12}H_{25}$), and free-base phthalocyanine (Pc) derivative.

Alternating multilayer films of PDI12 and Pc were prepared by horizontal dipping (LS method) of the Langmuir film. The energy transfer processes between PDI12 and Pc films are studied in detail by optical spectroscopic methods, including steady-state absorption and fluorescence, and time-resolved fluorescence in nanosecond timescale.

2. Experimental section

2.1. Materials

The symmetric trialkylphenyl-functionalized perylene diimide derivative (PDI12) was synthesized as reported previously [5]. The synthesis of 1,4,8,11,15,18-hexabutoxy-23-[3-(hydroxymethyl)phenoxy]phthalocyanine, Pc, is reported elsewhere [26]. Structures of the perylene diimide derivative (PDI12), and free-base phthalocyanine (Pc) are presented in Fig. 1. Octadecyl amine (ODA, Aldrich) was used without further purification. ODA and Pc were dissolved in chloroform (Merck) and PDI12 in hexane (Labscan Ltd.). Water was purified by MilliQ system (Millipore Corporation).

2.2. Film preparation

Surface pressure–mean molecular area isotherm measurements and film depositions by Langmuir–Schäfer or Langmuir–Blodgett methods were done using LB 5000 and minialternate systems from KSV Instruments (KSV Instrument Ltd., Helsinki, Finland). The subphase was a phosphate buffer containing 0.5 mM Na_2HPO_4 and 0.1 mM NaH_2PO_4 in MilliQ water. Samples for steady-state measurements were prepared on quartz plates which were cleaned by using the standard procedure [16]. The samples for fluorescence lifetime microscopy (FLM) measurements were prepared on one side of microscope cover glasses. These glasses were cleaned in ultrasonic bath with chloroform (30 min) and then in 0.001 M NaOH (30 min).

Before deposition of the photo-active layers, three layers of ODA were deposited on quartz plates using a standard Langmuir–Blodgett method [16]. This was done in order to prepare substrates with hydrophobic surfaces, required for deposition of photo-active layers by Langmuir–Schäfer method [17]. The PDI12 compound was dissolved in hexane at concentration of 0.1 mM and Pc compound was dissolved in chloroform at concentration of 0.25 mM. Deposition pressures for monolayers of PDI12 and Pc were 8 mN m^{-1} and 15 mN m^{-1}, respectively. Drying time of the films after every deposition was 1 min under nitrogen flow. When required, the PDI12 and Pc layers were separated by 2, 4, 6, or 8 ODA layers deposited by LB method.

2.3. Spectroscopic measurements

The steady-state absorption and emission spectra of the samples were recorded using Shimadzu UV-3600 UV–vis–NIR spectrophotometer and Fluorolog-3 (Spex Inc.) fluorimeter. The emission spectra were corrected applying correction function supplied by the manufacturer. Measurements were carried out at room temperature and ambient conditions.

Pump–probe technique was used for time-resolved measurements of the sample absorption. The instruments and the data analysis procedure have been described earlier [18]. Briefly, the transient absorption measurements with the pump–probe method were done using excitation at 500 nm. The wavelength of 500 nm was achieved by using an optical parametric amplifier (CDP 2017, CDP Inc., Russia) after multipass femtosecond amplifier and mixing fundamental harmonic with signal beams of the parametric amplifier. A typical time resolution of the instrument was 150 fs (FWHM) and other details can be found in the Supporting Information.

2.4. Fluorescence lifetime microscopy (FLM) measurements

Fluorescence lifetime images were acquired by inverse time-resolved fluorescence microscope MicroTime-200 (PicoQuant GmBH). The excitation wavelength, the spatial resolution, and the time resolution were 405 nm, 0.3 μm, and 60–70 ps, respectively. The manufacturer's software was used to calculate the lifetime map images.

3. Results

3.1. Film preparation

The formation and deposition of PDI12 Langmuir monolayers were described previously [6]. The isotherm for 100 mol % Pc is presented in Fig. 2. The shape of isotherm for 100 mol % Pc was typical for the expanded monolayers, with reasonable mean molecular area values, ca. 100 Å^2.

In order to study steady-state quenching, PDI12, Pc, and PDI12|Pc mono- and bi-layer samples were prepared. The bi-layer sample consisted of one LS monolayer of PDI12 on the bottom and Pc on the top of film. Fluorescence lifetime microscopy (FLM) measurements were performed for LS monolayers of PDI12 and Pc, and samples with PDI12 and Pc layers separated by 0, 2, 4, 6 and 8 layers of octadecylamine (ODA), and with the films deposited onto microscope cover glass substrates (0.1 mm thickness) to allow the use of immersion objective. At least two samples with the same number

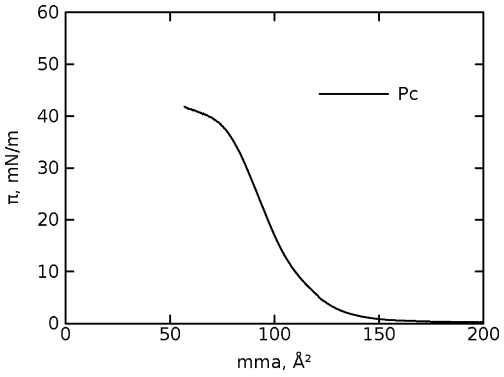

Fig. 2. Isotherm of 100 mol % Pc.

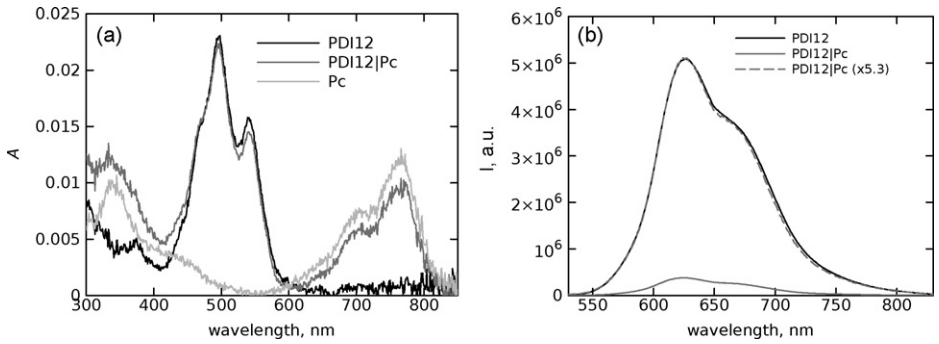

Fig. 3. (a) The absorption spectra of PDI12 (black line), Pc (grey line), and PDI12|Pc (light grey line) and (b) emission spectra of PDI12 (black line), PDI12|Pc (light grey line), and PDI12|Pc multiplied by 5.3 (dashed light grey line) mono- and bi-layer films on quartz plate. Excitation wavelength was 490 nm.

of intermediate ODA layers were prepare to check reproducibility of the results.

3.2. Absorption and emission spectra

Fig. 3a presents the absorption spectra of the PDI12, Pc, and PDI12|Pc mono- and bi-layer films. Several authors have studied the absorption and fluorescence properties of the perylene derivative films in detail [3–5]. Perylene diimides (PDI) derivatives, similar to PDI12, have intense absorption bands in the 400–600 nm region and an excimer-like emission band in the 500–800 nm region [3–5,25]. PDI12 is strongly aggregated in films, which can be observed from the steady-state absorption and emission spectra (Fig. 3) [5,6,10].

In LS films especially the Q-band of Pc is broad, and covers the region between 650 nm and 800 nm (Fig. 3a). This broadening of the bands for phthalocyanine compounds in thin films arises from aggregation [27,28]. Steady-state absorption spectrum of the double layer sample corresponds well to the sum of the spectra of the individual layers (Fig. 3a) indicating that there is no significant interaction between PDI12 and Pc in the ground state and the layers can be successfully deposited one on top of the other.

The emission spectra of the PDI12 and PDI12|Pc mono- and bi-layer films are presented in Fig. 3b. The samples were excited at 490 nm. The emission maximum of PDI12 is at 630 nm. No emission is seen in the phthalocyanine film due to self-quenching of the aggregated molecule, even though these compounds show clear emission when measured in solution [26]. This is, however, well established property of Pc films and was reported previously [29].

The fluorescence of PDI12 is strongly quenched in the presence of Pc in the adjacent layer (Fig. 3b). Nevertheless, the normalized emission spectra of PDI12 and bi-layer samples have virtually identical shapes. The quantum efficiency of energy transfer, ϕ_{ET}, can be expressed using the ratio of the quantum yields of the donor in the presence (ϕ) and absence (ϕ_0) of the acceptor, or using the fluorescence lifetimes as [30]

$$\phi_{ET} = 1 - \frac{\phi}{\phi_0} = 1 - \frac{\tau}{\tau_0}, \quad (1)$$

where τ is the emission lifetime of PDI12|Pc sample, and τ_0 is the lifetime of unquenched PDI12 layer. The energy transfer quantum yield can be estimated from relative intensities of emission. In steady-state fluorescence measurements, the integrated emission intensity (500–800 nm) of bi-layer PDI12|Pc sample is only 7% of the intensity of PDI12 monolayer sample. This means that 93% (ϕ_{ET}) of photoexcited states of PDI12 decay via the energy transfer from PDI12 to Pc layers.

3.3. Pump–probe measurements

Time-resolved absorption measurements are useful in tracking species formed during relaxation of the photoexcitation. In particular, different intermediate state can be discriminated based on their characteristic spectral features. The pump–probe measurements require high absorbance of the samples and therefore multilayer films of PDI12 and PDI12|Pc were prepared (Fig. S1 in the Supporting Information) [31,32]. Similar measurements were carried out recently for a multilayer structures formed by a PDI derivative and phthalocyanine–fullerene dyad [25]. These measurements have shown that primary excited PDI molecules transfer the energy to phthalocyanine part of the dyad, which follows by a quick charge separation in the phthocyanine–fullerene layer. Experimentally this is seen as gradual change in the shape of the transient absorption spectrum measured by pump–probe method within few tens of picosecond. In a contrast, pump–probe measurements have not revealed any significant changes in the shape of the transient absorption spectrum of PDI12 upon addition of adjacent

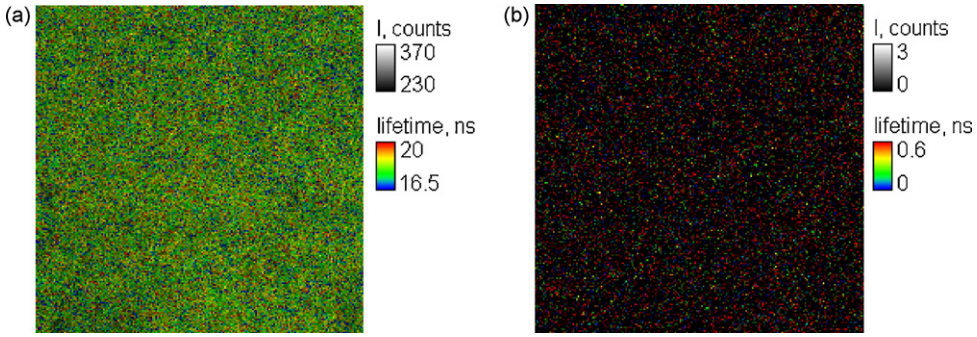

Fig. 4. FLM images of (a) PDI12 and (b) Pc monolayer films on a microscope cover glass substrate. The color scales represent average lifetimes and the total numbers of counts are indicated by color density at each point. The scan size is 20 μm. (For interpretation of the references to color in this figure legend, the reader is referred to the web version of this article.)

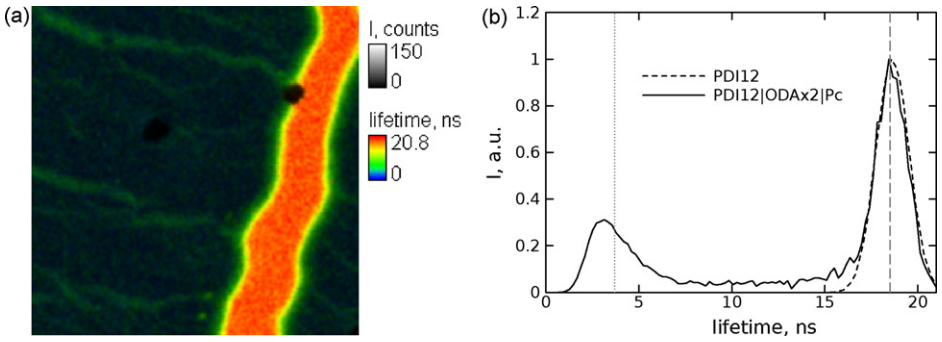

Fig. 5. FLM image of (a) sample with PDI12 and Pc layers separated by two layers of octadecylamine (ODA) on a microscope cover glass substrate. The scan size is 20 μm. The red strip in (a) is an example of broken Pc layer on top of film. (b) Distributions of average lifetimes for same sample (from FLM image (a), solid black line) and PDI12 monolayer film sample (from FLM image (a), dashed black line). The dotted and dashed grey lines show the average lifetimes at 3.7 ns and 18.5 ns, respectively. (For interpretation of the references to color in this figure legend, the reader is referred to the web version of this article.)

Pc layer, though the relaxation of the PDI12 excited state is apparently faster in the latter case (see Figs. S2 and S3 in the Supporting Information). This rules out the charge transfer between the layers a reason for PDI12 excited state quenching in bi-layer structures.

3.4. Fluorescence lifetime microscopy

Fig. 4 presents the FLM images of PDI12 and Pc monolayer films with uniform surface morphology over the scanned area, 20 μm × 20 μm. It should be noted, that the emission intensity and lifetime of Pc layer on the glass alone are much lower and shorter, respectively, than those of PDI12 layer on the glass, at least by few orders in magnitude. Therefore the FLM images obtained for bi-layer PDI12|Pc film are actually fluorescence maps of the PDI12 layer on the glass.

Fig. 5a presents the FLM images of sample with PDI12 and Pc layers separated by two layers of octadecylamine (ODA). The film contains broken structure, which comes from imperfect deposition of the Pc layer. The FLM image of PDI12|ODAx2|Pc film (Fig. 5a) shows two areas with different fluorescence properties of the PDI12 layer. The areas differ in both fluorescence intensity and lifetime. The lifetime distribution is shown in Fig. 5b, where two clear bands can be seen. Each area is rather uniform in itself. The bigger area has much shorter lifetime than the smaller one. The average lifetime of the bigger area is 3.7 ns, whereas the smaller part has a lifetime close to 18 ns, which match well with the lifetime of PDI12 layer alone. Intensity of the emission is virtually the same as that of PDI12 monolayer (Fig. 4a). Therefore a reasonable explanation for the morphology is that the most part of PDI12 layer is covered by the Pc layer and its emission is quenched. The red strip in Fig. 5a is an example of broken Pc layer on top of film. The average lifetime for this area is 18.5 ns. This lifetime is identical with PDI12 monolayer film sample average lifetime (Fig. 4a)

3.5. Fluorescence lifetimes and distance dependence

An increasing number of ODA layers was added between PDI12 and Pc monolayers in order to study dependence of the energy transfer on the distance between the donor and acceptor layers. The thickness of a single ODA layer was assumed to be the same as that of stearic acid layer, 2.4 nm [16]. The distance between the PDI12 and Pc layers, d, was calculated as the product of number of ODA layers and thickness of single layer, 2.4 nm. Utilization of FLM has allowed us to calculate emission decays for defect free areas. For example, darker parts in Fig. 5a were used to calculate cumulative emission decays, which were fitted and analyzed.

Table 1
Typical decay fit results. d is the distance between the donor and acceptor layers (number of ODA layers multiplied by 2.4 nm), τ is the lifetime, β is the stretching parameter as given by Eq. (2), the stretched exponential fit of goodnesses, and the weighted mean square deviations (χ^2) obtained from ordinary fitting procedure.

Sample	d (nm)	τ (ns)	β	χ^2
PDI12	–	18.53 ± 0.12	0.836 ± 0.004	1.056
PDI12|ODAx8|Pc	19.2	16.56 ± 0.09	0.822 ± 0.004	1.134
PDI12|ODAx6|Pc	14.4	15.32 ± 0.08	0.828 ± 0.003	1.172
PDI12|ODAx4|Pc	9.6	10.70 ± 0.05	0.829 ± 0.004	1.074
PDI12|ODAx2|Pc	4.8	3.74 ± 0.04	0.758 ± 0.005	1.180
PDI12|Pc	0	1.07 ± 0.02	0.642 ± 0.007	1.069

The decays were non-exponential, as can be expected for solid films. To deal with this problem, a stretch exponent model was proposed and successfully used to model excited state relaxation [25,33–35]. This model will be discussed later. Typical fit results are presented in Table 1. Also the actual number of analyzed data was greater since few samples were prepared for the same distances between the layers and four different unbroken areas (see Fig. 5a) were taken from each sample to generate decay curves. Table 1 presents also the stretching parameter, β, and the weighted mean square deviations (χ^2).

Fig. 6 presents the emission decays of PDI12 monolayer, PDI12|Pc bi-layer, and samples with PDI12 and Pc layers separated by four and two layers of octodecylamine (ODA). One important observation is that there is no “long tail” in the emission decay for PDI12|Pc bi-layer, which presents in the measurements carried

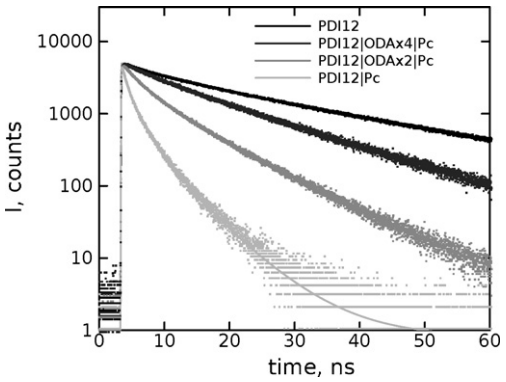

Fig. 6. Emission decays PDI12 monolayer, PDI12|Pc bi-layer, and samples with PDI12 and Pc layers separated by four and two layers of octadecylamine (ODA). Solid lines show stretched exponential fits of the data. The excitation wavelength was 405 nm.

out using traditional (macroscopic) time-correlated single photon counting techniques [6].

Ideally, the ratio of integral fluorescence intensities of quenched and unquenched PDI12 layers should be equal to the ratio of the lifetimes (see Section 3.2). However, the lifetimes were calculated excluding defected parts of the films, whereas no such procedure could be done for a standard fluorescence measurements. As a result the ratio of intensities always underestimate the quenching, e.g. for PDI12|Pc sample the relative intensity is 7% whereas the relative lifetime is 5.8%. The lifetimes were used to evaluate energy transfer efficiencies, as these values are considered to be more reliable.

4. Discussion

In polar solvents the fluorescence decays of PDI12 are mono-exponential and independent of the monitoring wavelength. The fluorescence lifetime varies from 3 ns to 4 ns. In nonpolar solvents, such as hexane, and at high concentrations, the emission shifts gradually to the red, the shorter 3 ns component disappears, and emission consists purely of the long-living, about 40 ns, component, which is assigned to the aggregates [5,6,10]. The fluorescence lifetime of PDI12 film is also long in the absence of acceptor (Table 1) and it is similar to that of the long-lived component in concentrated hexane solution [5,6,10]. Therefore, PDI12 seems to be fully aggregated in the LS film.

Simple mono-exponential fit of the PDI12 film fluorescence data yielded lifetime of 19.4 ± 0.6 ns. The result was unacceptable as the decay is clearly not mono-exponential, and the fit goodness was $\chi^2 = 1.90$. A better approximation has been achieved using bi-exponential fit. The fit lifetimes were $\tau_1 = 8.2 \pm 0.3$ ns and $\tau_2 = 25.9 \pm 0.24$ ns, and the fit goodness was $\chi^2 = 1.37$. The calculated average lifetime, using bi-exponential fit, was $\tau_{av} = 18.9$ ns. Even though decays are not mono- or bi-exponentials and a multiexponential fit could be used in order to obtain a reasonable approximation [36], the multiexponential decay model has no physical meaning, that is, the population of the excited states decreases non-exponentially due to inhomogeneity of the local environments of individual PDI12 molecules in the film.

The non-exponential behavior of organic molecules in solid films, especially in bi-layer films, is a well known phenomenon [36,37]. The stretch exponential model describes this kind of behavior quite well [33–35]. It has sharper decay at the beginning and slower relaxation at the end, as presented in Fig. 6. In the present study a better approximation, as presented in Table 1, has been achieved using the stretch exponential fit. The fit function is

$$I(t) = I_0 \exp\left[-\left(\frac{t}{\tau}\right)^{\beta}\right], \tag{2}$$

where τ is the emission lifetime and β is an empirical parameter that shows the degree of heterogeneity present. Parameter β has value in the range from 0 to 1, and $\beta = 1$ corresponds to pure exponential decay (no distribution of the states) and decrease in β means increase in distribution width. Eq. (2) is an analytical finding and there is no exact mathematical expression linking β with the distribution width or the type of distribution. However, it can serve as a reasonable mathematical model to estimate the emission lifetime, τ, from non-exponential decays. In other words, the stretched exponential can be used to analyze complex fluorescence decays with different emission sources in different microenvironments, which can lead to a distribution of decay times.

In PDI12|Pc films non-exponential behavior is usually attributed to the distribution of orientations and distances between the donor and acceptor molecules. The stretched exponential function not only describes the decay profiles almost exactly, but also derives from the more realistic decay model of continuous lifetime distributions in PDI12|Pc films, rather than from an arbitrary assumption of single or multiple discrete exponential decay components. Moreover, this approach yields, besides the mean lifetime τ of the distribution, an additional parameter of interest (β), which is related to the width of the lifetime distribution and which is a direct measure for the local heterogeneity of the sample. The heterogeneity parameter is important because it enables the study mechanisms that cause a lifetime distribution to broaden (β value decreases) or narrow (β value increases), as presented in Table 1 and Fig. 5b. In Table 1, β value decreases when distance between active layers gets shorter, this decrease is due to the inhomogeneity which comes from imperfect deposition of the Pc layer.

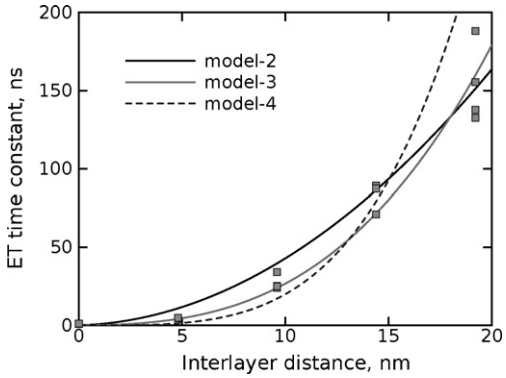

Fig. 7. Energy transfer time constant as a function of distance between PDI12 and Pc layers in the films. The model with $n = 2$ yields $R_0 = 6.9$ nm and $d_0 = 0.5$ nm, with $n = 3$ yields $R_0 = 10.0$ nm and $d_0 = 1.3$ nm, and with $n = 4$ yields $R_0 = 10.5$ nm and $d_0 = 0.7$ nm, respectively.

Energy transfer time constant, as a function of distance between PDI12 and Pc layers in the films, is shown in Fig. 7. The energy transfer time constant, τ_{ET}, can be obtained from the measured emission lifetimes, τ, and the lifetime of unquenched PDI12 layer, τ_0, as

$$\tau_{ET} = \left(\tau^{-1} - \tau_0^{-1}\right)^{-1} \tag{3}$$

As can be seen from Eq. (3), τ_0 has a big influence on determination of the energy transfer time constant, τ_{ET}. The experimental lifetime, τ_0, was taken from an average of several measurements of lifetime obtained using FLM. The energy transfer time constants have large dispersion, as indicated by the noticeable errors in Fig. 7, especially when τ and τ_0 are close to each other. Such large dispersion is not only due to the limitations in measuring the lifetimes, but also due to the possible interpenetration among the LS film layers, which brings uncertainties as to the precise distance between donor and acceptor layers.

Förster theory can be applied to the study of energy transfer [21,38–40]. Fluorescence quenching in LS monolayer film by energy transfer can be described by the following equation [41–43]

$$\tau_{ET} = \tau_0 \left[\frac{d + d_0}{R_0}\right]^n, \tag{4}$$

where d is the distance between the donor and acceptor layers, i.e. thickness of intermediate ODA layers, d_0 is the distance between the donor and the acceptor molecules without separating ODA layers, i.e. the acceptor layer is deposited on top of the donor layer, R_0 is the Förster radius, and n is the parameter which identifies the model. When the energy is transferred between two isolated dipoles $n = 6$ [38]. However, the power dependence of the energy transfer is greatly influenced by the geometry of the system [41]. In the case of energy transfer from a point dipole to a layer, $n = 4$, and in layer to layer energy transfer $n = 2$ [40]. Given a Förster energy transfer mechanism, $n = 3$ distance dependence is consistent with resonance electronic energy transfer from

a two-dimensional donor layer to a three-dimensional array of acceptors [42]. The results of the distance dependence fits for $n = 2$, $n = 3$, and $n = 4$ are presented in Fig. 7. The model with $n = 2$ yields $R_0 = 6.9$ nm and $d_0 = 0.5$ nm, with $n = 3$ yields $R_0 = 10.0$ nm and $d_0 = 1.3$ nm, and with $n = 4$ yields $R_0 = 10.5$ nm and $d_0 = 0.7$ nm, respectively. The second and third order dependences give somewhat better approximation of the results than fourth order dependence (Fig. 7), and can be used to compare the energy transfer in PDI12|Pc films. Results with similar molecular structures have already been published [21,40,43].

Hill et al. reported a second order distance dependence for layered Langmuir–Blodgett polymer structure, consistent with energy transfer between two fluorescent polymers in monolayers. They used poly(9,9-dioctylfluorene-co-benzothiadiazole) as an acceptor and poly(9,9-dioctylfluorene) as a donor, and calculated that the critical distance was 3.8 nm [40]. A third order distance dependence of the transfer rate between the excited donor and the acceptor film was assumed by Shaw et al. [43]. They used poly(3-hexylthiophene) as the acceptor layer and poly[(9,9-dioctylfluorenyl-2,7-diyl)-co-(1,4-benzo-{2,1′,3}-thiadiazole)] as the donor layer, and observed the critical distance to be ∼12 nm. In the present study, both the second and third order model predictions are in good agreement with the experimental measurements.

Energy transfer between two layers is chosen here, because perylene diimide derivative and phthalocyanine layers in LS films are probably organized close to each other and behave more as a film than as single dipoles. Therefore estimated distance dependence of the interlayer energy transfer, using the second power approach, has shown critical distance to be 6.9 nm and $d_0 = 0.5$ nm. This result suggests that energy transfer occurs from a donor layer to a acceptor layer. The result is in good agreement with the value founded by Del Caño et al. [21] for LB monolayers of phthalocyanine and perylene derivative. From they observation, using the fourth power dependence, the estimated critical distance was $R_0 = 8.4$ nm. According to their results a slightly greater value of the energy transfer distance, than reported in this work, is probably explained by small number of experimental points available for the estimation. However, when varying the model (Fig. 7) and thus the power dependence of the energy transfer rate the exact calculation of R_0 and d_0 also differs.

5. Conclusions

The interaction between perylene diimide derivative and phthalocyanine films was studied by steady-state and time-resolved optical measurements. The energy transfer from the perylene diimide derivative to the phthalocyanine chromophore is attributed to be the main relaxation process of the excited PDI12 in the PDI12|Pc structure. The non-exponential behavior of organic molecules in solid films is a well known phenomenon. To deal with the problem, a stretch exponent model was successfully used to fit emission decay data. In addition, we have demonstrated that the time constant for the energy transfer between perylene diimide derivative and phthalocyanine layers follows roughly second order distance dependence. This energy transfer mechanism is consistent with the resonance electronic energy transfer from a donor layer to an acceptor layer, yielding a value of 6.9 nm for the critical transfer distance.

Acknowledgment

This work was supported by the Academy of Finland.

Appendix A. Supplementary data

Supplementary data associated with this article can be found, in the online version, at doi:10.1016/j.jphotochem.2010.01.017.

References

[1] C.W. Tang, Appl. Phys. Lett. 48 (1986) 183.
[2] S. Günes, H. Neugebauer, N.S. Sariciftci, Chem. Rev. 107 (2007) 1324.
[3] W.E. Ford, P.V. Kamat, J. Phys. Chem. 91 (1987) 6373.
[4] A.K. Dutta, K. Kamada, K. Ohta, Langmuir 12 (1996) 4158.
[5] Z. Chen, V. Stepanenko, V. Dehm, P. Prins, L.D.A. Siebbeles, J. Seibt, P. Marquetand, V. Engel, F. Würthner, Chem. Eur. J. 13 (2007) 436.
[6] A. Tolkki, E. Vuorimaa, V. Chukharev, H. Lemmetyinen, P. Ihalainen, J. Peltonen, F. Würthner, Langmuir (2009), doi:10.1021/la903978y.
[7] T. Abe, S. Ogasawara, K. Nagai, T. Norimatsu, Dyes Pigments 77 (2008) 437.
[8] F. Würthner, Chem. Commun. 14 (2004) 1564.
[9] E.L. Nordgård, E. Landsem, J. Sjöblom, Langmuir 24 (2008) 8742.
[10] R.F. Fink, J. Seibt, V. Engel, M. Renz, M. Kaupp, S. Lochbrunner, H.-M. Zhao, J. Pfister, F. Würthner, B. Engels, J. Am. Chem. Soc. 130 (2008) 12858.
[11] T. Nojiri, M.M. Alam, H. Konami, A. Watanabe, O. Ito, J. Phys. Chem. A 101 (1997) 7943.
[12] J. Zhou, J. Mi, R. Zhu, B. Li, S. Qian, Opt. Mater. 27 (2004) 377.
[13] G. de la Torre, C.G. Claessens, T. Torres, Chem. Commun. 437 (2007) 2000.
[14] Z. Bao, A.J. Lovinger, A. Dodabalapur, Appl. Phys. Lett. 69 (1996) 3066.
[15] J. Blochwitz, M. Pfeiffer, T. Fritz, K. Leo, Appl. Phys. Lett. 73 (1998) 729.
[16] G. Roberts, Langmuir–Blodgett Films, Plenum Press, New York, 1990.
[17] T. Charitat, E. Bellet-Amalric, G. Fragneto, F. Graner, Eur. Phys. J. B 8 (1999) 583.
[18] N.V. Tkachenko, L. Rantala, A.Y. Tauber, J. Helaja, P.H. Hynninen, H. Lemmetyinen, J. Am. Chem. Soc. 121 (1999) 9378.
[19] Y. Ohmori, E. Itoh, K. Miyairi, Thin Solid Films 499 (2006) 369.
[20] M. Hiramoto, H. Fukusumi, M. Yokoyama, Appl. Phys. Lett. 61 (1992) 2580.
[21] T. Del Caño, M.L. Rodrígues-Méndez, R. Aroca, J.A. De Saja, Mater. Sci. Eng. C 22 (2002) 161.
[22] R. Schüppel, T. Dienel, K. Leo, M. Hoffmann, J. Lumin. 110 (2004) 309.
[23] M.S. Rodríguez-Morgade, T. Torres, C. Atienza-Castellanos, D.M. Guldi, J. Am. Chem. Soc. 128 (2006) 15145.
[24] P. Vivo, M. Ojala, V. Chukharev, A. Efimov, H. Lemmetyinen, J. Photochem. Photobiol. A: Chem. 203 (2009) 125.
[25] H. Lehtivuori, T. Kumpulainen, M. Hietala, A. Efimov, H. Lemmetyinen, A. Kira, H. Imahori, N.V. Tkackenko, J. Phys. Chem. C 113 (2009) 1984.
[26] E. Sariola, A. Kotiaho, N.V. Tkachenko, H. Lemmetyinen, A. Efimov, J. Porph. Phth. (in press).
[27] A.K. Ray, A.V. Nabok, A.K. Hassan, O. Omar, R. Taylor, M.J. Cook, Philos. Mag. B 78 (1998) 53–64.
[28] P.-l. Chen, D.-h. Tang, X.-b. Wang, H. Chen, M.-h. Liu, J.-b. Li, X.-h. Liu, Colloids Surf. A: Physicochem. Eng. Asp. 175 (2000) 171–178.
[29] Y. Sakakibara, R.N. Bera, T. Mizutami, K. Ishida, M. Tokumoto, T. Tani, J. Phys. Chem. B 105 (2001) 1547–1553.
[30] B. Valeur, Molecular Fluorescence, Wiley-VCH, Weinheim, 2002.
[31] H. Lehtivuori, A. Efimov, N.V. Tkachenko, H. Lemmetyinen, Chem. Phys. Lett. 437 (2007) 238–242.
[32] H. Lehtivuori, T. Kumpulainen, A. Efimov, H. Lemmetyinen, A. Kira, H. Imahori, N.V. Tkackenko, J. Phys. Chem. C 112 (2008) 9896–9902.
[33] C.P. Lindsey, G.D. Patterson, J. Chem. Phys. 73 (1980) 3348.
[34] D. Pevenage, M. Van der Auweraer, F.C. De Schryver, Langmuir 15 (1999) 4641.
[35] M.N. Berberan-Santos, E.N. Bodunov, B. Valeur, Chem. Phys. 315 (2005) 171.
[36] B.B. Postacchini, V. Zucolotto, F.B. Dias, A. Monkman, O.N. Oliveira Jr., J. Phys. Chem. C 133 (2009) 10303.
[37] K. Ray, H. Nakahara, A. Sakamoto, M. Tasumi, Chem. Phys. Lett. 342 (2001) 58.
[38] T. Förster, Discuss. Faraday Soc. 27 (1959) 7.
[39] N.J. Turro, Modern Molecular Photochemistry, University Science Books, Mill Valley, CA, 1991.
[40] J. Hill, S.Y. Heriot, O. Worsford, T.H. Richardson, A.M. Fox, Phys. Rev. B 69 (2004) 041303.
[41] H. Kuhn, J. Chem. Phys. 53 (1970) 101.
[42] D.R. Haynes, A. Tokmakoff, S.M. George, J. Chem. Phys. 100 (1994) 1968.
[43] P.E. Shaw, A. Ruseckas, I.D.W. Samuel, Phys. Rev. B 78 (2008) 245201.